J. Membrane Biol. 125, 1–11 (1992)

The Journal of
Membrane Biology

Depolarization Exposes the Voltage Sensor of the Sodium Channels to the Extracellular Region

Marei Sammar†‡, Gad Spira‡§, and Hamutal Meiri†§*

†Department of Physiology and Biophysics and ‡Laboratory of Cell Biology, The Faculty of Medicine, and §The Rappaport Family Institute for Research in the Medical Sciences, Technion-Israel Institute of Technology, Haifa 31096, Israel

Summary. Two domains of Na channels were mapped with site-specific antibodies raised in rabbit against synthetic peptides corresponding to a part of the voltage sensor of internal repeat 1 – C_1^+ (amino acids 210–223) and to a region designated dipole (amino acids 1690–1699) of eel electroplax sodium channels. The antibodies bind to their respective domains in both purified and membrane-bound channels and immunoprecipitate the channels from eel electroplax and rat brain synaptosomes.

Anti-C_1^+ depresses the action potential of rat sciatic nerve in a concentration-dependent way. It binds to the external side of rat brain synaptosomal vesicle, and its binding is potentiated by depolarization. Anti-dipole binds to the inner side of the vesicle, and the binding is inhibited by depolarization.

Key Words sodium channels · antibodies to synthetic peptides · immunoprecipitation · eel electroplax · rat brain synaptosomes

Introduction

The voltage-sensitive sodium channels mediate the initial rapid increase in sodium permeability, which is responsible for the rising phase of the action potential in most multicellular organisms (Hodgkin & Huxley, 1952; Armstrong, 1981; Hille, 1984; Bezanilla, 1985; Aldrich & Stevens, 1987). Sodium channels have been purified from many excitable tissues (Lombet & Lazdunski, 1984; Agnew, Rosenberg & Tomiko, 1986; Levinson et al., 1986; Barchi, 1988; Catterall, 1988). Molecular cloning and sequencing yielded several cDNA clones encoding for the primary structure of the alpha subunit from eel electroplax (Noda et al., 1984), rat brain (Noda et al., 1986*a*,*b*; Kayano et al., 1988; Suzuki et al., 1988), rabbit skeletal muscle (Caldwell & Schaller, 1989; Trimmer et al., 1989; Kallen et al., 1990), *Drosophila* brain (Salkoff et al., 1987; Ganetzki & Loughney, 1989) and TTX-resistant rat heart Na channel (Rogart et al., 1989). Each is comprised of 1820–2100 amino acids. Analysis of homology matrix among linear sequences demonstrates the presence of four internal repeats within the primary structure of each channel and the existence of 6–8 transmembrane segments in each repeat (Greenblatt, Blatt & Montal, 1985; Guy & Seetharamulu, 1986; Noda et al., 1986*a*; Trimmer et al., 1989). The region between repeats 1 and 2 was found to be the major region of phosphorylation (Rossie, Gordon & Catterall, 1987). The external strand between segment 5 and 6 of internal repeat 1 carries several glycosylation sites (Catterall, 1988) and has the binding sites for scorpion toxin (Catterall, 1990) and tetrodotoxin (Catterall, 1990; Stuhmer, 1990). The C-terminus (amino acids 1781–1794, Gordon et al., 1987) and the region between internal repeats 2 and 3 were found to be intracellular (Gordon et al., 1988). The region between internal repeats 3 and 4 was found to be intracellular and responsible for inactivation (Vassilev, Scheur & Catterall, 1988; Stuhmer et al., 1989).

Several models suggest particular channel folding to account for channel gating (Noda et al., 1984, 1986*a*; Greenblatt et al., 1985; Kosower, 1985, 1991; Guy & Seetharamulu, 1986; Catterall, 1988, 1990). All these models suggest that the ampiphilic segment S_4 participates in voltage gating. This segment consists of a unique arrangement of positively charged amino acids (arg^+ and lys^+) at each third position and two nonpolar amino acids intervening between them (Noda et al., 1984, 1986*a*,*b*). Organized as a C_{10} helix (Noda et al., 1984, 1986*a*,*b*; Kosower, 1985, 1991) or as an alpha helix (Noda et al., 1984; Catterall, 1988), the S_4 may form a vertical strip of positive charges. All models mentioned above postulated that at rest the positive charges on S_4 are balanced by negative charges of other transmembrane strands, thus forming an array of dipoles, and that the movement of the positive charges on S_4 in response to membrane depolariza-

* *Address for correspondence:* 11 Achimeir St., #3, Ramat Aviv Gimel, Tel Aviv 69126, Israel.

tion deforms the array of dipoles, thereby gating the channel (Noda et al., 1984, 1986*a*; Greenblatt et al., 1985; Kosower, 1985; Guy & Seetharamulu, 1986; Catterall, 1988). Point mutations in the S_4 region have shown that replacing the charged amino acid lysine in the middle of this strand with the neutral amino acid glutamine shifts the voltage-dependent channel activation and, in some cases, reduces the slope of the voltage dependency. Replacing lysine with the negatively charged amino acid glutamate reduces the steepness of the slope of the voltage dependency of activation even more (Stuhmer et al., 1989). Yet, the S_4 segment of internal repeat 1 is accessible to its site-specific antibodies when applied from the external and not from the internal side of the membrane (Meiri et al., 1987; Meiri, Sammar & Schwartz, 1989; Schwartz, Palti & Meiri, 1990). Recently Guy and Conti (1990) proposed the "propagating helix model," which suggests that the first four of the charged amino acids of each S_4 segments (the ones closer to the outside) are moving externally upon depolarization. Thus, the topography of the S_4 region and its exposure to the extracellular solution during depolarization require a detailed examination.

Antibodies were raised in rabbit against two peptides: C_I^+ (amino acids 210–223, eel channel numbering), which corresponds to the S_4 segment of internal repeat 1, and dipole (amino acids 1690–1699), next to the C-terminus, for which the larger dipole moment for the entire sodium channel sequence was calculated (Y. Palti, *unpublished*).

We address in this paper the following questions: (i) What is the topography of these domains as opposed to membrane sideness? (ii) What is the influence of membrane depolarization on the accessibility of these domains and does it confirm the propagating helix model of Guy and Conti (1990)?

Materials and Methods

Crude Electroplax Membrane Fractions (EMF)

Electroplax membranes were prepared as described by Duch and Levinson (1987). A stored organ was partially thawed, sliced and homogenized in grinding buffer [50 mM sodium phosphate, 5 mM EDTA, 0.1 mM phenyl-methylsulfonyl fluoride (PMSF), pH 6.8]. The homogenates were centrifuged, resuspended in grinding buffer and centrifuged again, and the pellet was resuspended in 1 ml grinding buffer/g pellet. All steps were conducted at 2°C. The EMF were stored at −140°C.

Membrane Solubilization

EMF were solubilized according to the methods of Duch and Levinson (1987). Stored EMF were thawed, solubilized by 10% (vol/vol) of 120 mM CHAPS, homogenized, and spun at 100,000 × *g* for 1 hr at 2°C. The supernatant containing the solubilized sodium channels (SEMF) was collected.

Partial Purification on DEAE

SEMF (9–10 ml) were mixed with equal volume of DEAE previously equilibrated overnight with ion exchange buffer [50 mM sodium phosphate, 200 mM NaCl, 10 mM CHAPS, 3 mg/ml asolectin (Sigma, St. Louis, MO), pH 6.8]. The resin was washed with ion exchange buffer, the ionic concentration was increased to 0.4 M, and the supernatant was collected. The process was repeated, and the second supernatant was combined with the first supernatant. The preparation was concentrated by ultrafiltration using an Amicon minidialyzer with a XM100 membrane.

Preparation of Crude Liver Membrane (CLM)

Rat liver was homogenized in membrane buffer (0.3 M mannitol, 1 mM EDTA, pH 7.4) and centrifuged twice. The pellet was resuspended and stored at −140°C. All steps were carried out at 4°C.

Preparation of Rat Brain Membrane (RBM)

According to Kanner (1980), rat brain was homogenized in membrane buffer and spun down. The pellet was loaded onto a Ficoll step gradient (2, 8, 16 and 20%) and centrifuged. The 8–16% interphases were collected, washed, and centrifuged. The synaptosomes were lysed with hypotonic buffer (5 mM EDTA, 10 mM Tris-Cl, pH 7.4) at 40/1 (vol/vol) ratio followed by centrifugation. The synaptic plasma membrane pellet was collected and stored at −140°C.

Calf Heart Sarcolemma (CHS)

According to the procedure of Reeves and Sutko (1979), calf heart was isolated fresh into imidazole buffer (0.3 M sucrose, 5 mM $MgSO_4$, 10 mM imidazole-HCl, pH 7.4), sliced and homogenized. The solution was further homogenized. Sucrose concentration was increased to 0.6 M, and the homogenate was centrifuged. The supernatant was collected and mixed at 1.5/1 (vol/vol) ratio with Tris-Mops buffer (160 mM NaCl, 20 mM Mops-Tris, pH 7.4) and centrifuged. Samples were suspended in Tris-Mops buffer and stored at −70°C.

Protein was determined using the Lowry et al. (1951) procedure.

Saxitoxin (STX) Binding

Saxitoxin binding was measured using [^{3}H]-STX (New England Nuclear, Boston, MA, specific activity of 37.3 Ci/mmol at 1 mCi/ml). Samples (100–200 μg/200 μl grinding buffer) were incubated at 5–10 nM [^{3}H]-STX for 60 min at 4°C. The reaction was terminated by washing with 3 ml of ice-cold grinding buffer followed by rapid filtration through Whatmann GF/C filters (membrane preparations) or GF/B filters (all other preparations) preincubated with 0.3% polyethylene amine (Bruns, Lawson-Wendling &

Pugsley, 1983). Specific binding was defined as the difference between radioactivity bound in the presence and absence of 1 μM tetrodotoxin (Duch & Levinson, 1987).

SDS-PAGE

Samples were dissolved in a sample buffer (10% glycerol, 3% sodium dodecyl sulfate (SDS), 5% 2-mercaptoethanol, 62.5 mM Tris-HCl, pH 6.8), incubated for 3 min in a water bath at 90°C, and loaded onto a 4–15% poly-acrylamid gradient SDS gel (Laemmli, 1970). Protein bands were visualized by silver staining (Wray et al., 1981).

Peptide Synthesis and Conjugation

Peptide synthesis was carried by the solid-phase method of Merrifield (1985). The petide was cleaved off the resin with anhydrous HF at 0°C, isolated, and purified by reverse-phase HPLC on a C_{18} column. The amino acid composition of the peptide was verified by amino acid analysis. The peptide was conjugated either to kehole limpet hemocyanin (KLH, Calbiochem, San Diego, CA) or to bovine serum albumin (BSA, Sigma) using EDCI [1-ethyl-3(3-dimethylaminopropyl) carbodiimide hydrochloride] (Sigma) as coupling reagent. The peptide-carrier conjugate was dialyzed overnight against excess PBS and kept at −20°C.

Immunization

Rabbits were immunized by multistage subcutaneous and intramuscular injections of 1 mg KLH-peptide conjugate emulsified in 0.5 ml Freund's complete adjuvant. Booster injections were given, if necessary, with Freund's incomplete adjuvant. The immunoglobulin fractions from whole serum were purified on a protein-A column.

ELISA Procedure

To measure the binding of anti-peptide antibody, flat-bottomed immunoplates (Nunc) were coated with 50 μl of 10 μg antigen/ml, blocked with 1% BSA, incubated with rabbit anti-serum (or its IgG fraction, purified on a protein-A column), and overlayed with alkaline phosphatase-conjugated goat anti-rabbit IgG. The reaction was developed with Sigma 103–104 substrate (1 mg/ml), and the optical density was measured at 405 nm.

IgG content was also determined by ELISA using standard IgG (courtesy of B. Gieger, The Weizmann Institute of Science, Rehovot, Israel).

Dot Blot

A dot of 5 μl (0.5–1 μg protein/ml) of antigen was adsorbed onto 1 × 1 cm nitrocellulose membrane (Schleicher & Schull D-3354, Dassel, FRG) followed by blocking of irrelevant sites with 5% (wt/vol) nonfat dry milk. Membranes were incubated with the antibodies, and detection of bound antibodies was achieved using ^{125}I-labeled protein-A.

Immunoprecipitation of Sodium Channels

RBM was diluted in a solubilization buffer containing 100 mM choline chloride, 10 mM EDTA, 10 mM EGTA, 50 mM potassium phosphate, pH 7.4, and 5% Triton X-100 containing 100 μM PMSF, 1 mM iodacetamid, and 1 μM pepstatin. Nonsolubilized membranes were precipitated by sedimentation at 8000 × g for 15 min.

The supernatant was incubated for 16 hr with the appropriate antibody (purified on protein-A), and the antibody-antigen complexes were isolated by adsorption onto protein-A-Sepharose.

Phosphorylation of Immunoprecipitated Na Channels

Following Gordon et al. (1987) immunoprecipitated samples were washed with phosphorylation buffer (5 mM $MgCl_2$, 5 mM EDTA, 25 mM HEPES-Tris, pH 7.4, and 0.1–0.5% Triton X-100). Phosphorylation was carried out according to Costa and Catterall (1984) using 500 ng of the catalytic subunit of cAMP-dependent protein kinase (Sigma) and 10 μCi of gamma[^{32}P]-ATP (New England Nuclear) for 1 min at 36°C. The reaction was terminated by ice-cold (4°C) buffer (100 mM sodium phosphate, pH 7.4, 20 mM EDTA, 50 mM KF, and 0.5% Triton X-100) followed by centrifugation. The pellet was washed (50 mM sodium phosphate, pH 7.4, 20 mM KF, 75 mM NaCl, 2.5 mM EDTA, 0.01% NaN_3, and 0.5% Triton X-100) and centrifuged, and samples were electrophoresed on SDS-PAGE. Autoradiography was done on Kodak XM-5 paper.

Preparation of Vesicles from Rat Brain Synaptosomal Membranes

Minicolumns were prepared according to Barzilai and Rahamimoff (1987) in 1-ml tuberculin syringes filled with Sephadex G-50 pre-equilibrated with either KPi medium (85 mM KCl, 10 mM TEA, 1 mM $MgSO_4$, 200 μM $CaCl_2$, 3 mM ATP, 1 μM TTX, 10 μM 4-AP, 5 mM potassium phosphate and 5 mM sodium phosphate, pH 7.4, osmolarity 225) or with NaPi medium (90 mM NaCl, 10 mM TEA, 1 μM TTX, 10 μM 4-AP, 1 mM $MgSO_4$, 3 mM ATP, 5 mM potassium phosphate and 5 mM sodium phosphate, pH 7.4, osmolarity 215). The syringes were centrifuged, and samples of RBM (200 μl containing 0.5 mg protein/ml) were loaded. Vesicles were collected at the bottom of the syringes following centrifugation.

Binding to RBM Vesicles

Binding to the external side of the vesicles was performed by incubating vesicles (3–5 μl containing 30–50 μg protein) for 1 hr at room temperature in 200 μl of a test medium containing 100 μg IgG. Antibodies bound to vesicles were detected by [^{125}I]-protein-A. Vesicles were also tested for [^{3}H]-STX binding as described above.

Binding to both membrane sides was done by perforating the vesicle at RT for 30 min with 0.05% saponin (Sigma). The vesicles were washed, and binding was performed as above.

To achieve binding to the internal side of the vesicles, the membranes were first incubated in internal medium (KPi or NaPi) containing antibodies for 1.5 hr; vesicles were eluted through minicolumns containing the antibodies. The outside

bound antibodies were blocked by incubation with protein-A at RT for 1 hr. The vesicles were lysed with hypotonic solution (5 mM EDTA, 10 mM sodium phosphate, pH 7.4) and incubated with [^{125}I]-protein-A. Specificity was determined by binding in the presence and absence of the corresponding peptides, and background was subtracted using normal rabbit IgG.

Measurements of Membrane Potentials of the RBM Vesicles

To measure the membrane potential of RBM vesicles, a voltage-dependent uptake of the lipophilic cation tetra-phenyl-phosphonium (TPP^+) was measured (Barzilai & Rahamimoff, 1987). The vesicles were loaded with KPi and diluted into a test medium buffer containing 0.035 mM TPP^+, 0.2 μCi/ml of [^{3}H]-TPP^+ and KPi buffer with different concentrations of KCl and with a balancing concentration of NaCl or of choline chloride. The amount of [^{3}H]-TPP^+ bound to the vesicles was measured following chromatography through a Dowx-50 minicolumn (Gasko et al., 1976). Membrane potential was calculated by the Nernst equation on the basis of the measured external and internal concentration of TPP^+. The internal concentration was determined by dividing the amount of TPP^+ inside the vesicles by their internal volume (determined as explained below).

The internal volume of the vesicles was measured by the [^{3}H]-glucose method (Barzilai & Rahamimoff, 1987). The trapped glucose in the vesicles was measured after a transfer of the vesicles through an identical Sephadex G_{50} column pre-equilibrated with glucose-free internal medium. No loss of [^{3}H]-glucose from the vesicles occurred in this procedure. The internal volume was 1.8–2.5 μl/100 μg protein.

RBM Vesicles Sealing

Vesicles were prepared after the RBM were equilibrated with NaPi containing 10 mM [^{22}Na]Cl (replacing equivalent amount of unlabeled NaCl) and eluted once through a column pre-equilibrated with radioactive sodium and twice through an identical column without radioactive sodium to ensure no ^{22}Na was bound to the outside of the vesicles.

Vesicles (3–5 μl containing 30–50 μg protein) were then diluted into 200 μl NaPi containing 5–85 mM NaCl and a balancing concentration of choline chloride. Following an incubation period, the vesicles were eluted through a Dowx-50 minicolumn, and the amount of ^{22}Na remained in the vesicles was determined. Alternatively, vesicles were preloaded with KPi containing 10 mM [^{86}Rb]Cl, and all steps were repeated with external KPi containing 5–85 KPi and balancing concentrations of choline chlorine.

Determination of Vesicles Sideness

The proportion of right-side out *vs.* inside-out vesicles was determined by binding of [^{3}H]-STX. First binding to the external side of the vesicles was performed (as described above). Then perforated vesicles were prepared by saponin treatment (*see above*). Toxin binding to perforated vesicles was performed like its binding to the external side of the vesicles. The ratio of binding to outside of intact vesicles *vs.* perforated vesicles was used as the first estimate of vesicle sideness. Direct binding to the vesicle inside was performed by equilibrating mini-columns with RBM and 5–10 mM [^{3}H]-STX for 60 min at 4°C, and elution once followed by elution twice through columns pre-equilibrated with internal medium and 1 μM TTX to ensure no [^{3}H]-STX was bound to the outside of the vesicle. Vesicles were filtered as described above for [^{3}H]-STX binding. Specificity was determined by adding 1 μM TTX to the first minicolumn. The ratio of binding to outside *vs.* inside of the vesicle was used as a second estimate of vesicle sideness.

Measurements of the Compound Action Potential

Rats were sacrificed by i.p. injection of pentobarbitone (50 mg/kg body wt), and both sciatic nerves were dissected-out, placed in a Ringer's solution (containing in mM: NaCl 154, KCl 5.6, $CaCl_2$ 1.2, and Tris-HCl 10, pH adjusted with 1 N NaOH to 7.4), desheathed, mounted onto a recording chamber and stimulated at 1 Hz. The compound action potential was recorded, stored digitally and plotted. All measurements were performed at room temperature. Antibody (Ig fraction after protein-A column) was perfused at a given concentration and allowed to equilibrate with the nerve for 20 min. Antibody preincubated with the peptide, normal rabbit IgG and irrelevant rabbit antibodies were used as controls. At super-maximal stimulation, the following parameters were measured: action potential amplitude, action potential duration at 50 and 90% amplitude, and conduction velocity. The threshold current was obtained from strength-duration curves.

Results

Sequence Analysis

The oligopeptides corresponding to amino acids 210–223 (C_I^+, eel channel numbering), and 1690–1699 (dipole) are shown at the top line of Fig. 1*A* and *B*. C_I^+ corresponds to a part of the S_4 segments of internal repeat 1 (Noda et al., 1984, 1986*a*) and has 86% homology with the corresponding region of rat brain sodium channels (Noda et al., 1984, 1986*a*,*b*) and 92% homology with skeletal muscle Na channel (Trimmer et al., 1989) (Fig. 1*A*). The homology of C_I^+ with the S_4 segments of repeat 4 (S_4IV of eel electroplax Na channel) is given in Fig. 1*C* (Noda et al., 1984, 1986*a*, *b*). It is shown that the structure of charged amino acids at every third position and two neutral amino acids in between is kept in both C_I^+ and S_4IV but the sequence homology is small. Dipole of eel electroplax has 60% homology with the corresponding domain in rat brain (Fig. 1*B*). The amino acid tryptophan (eel sequence 1698) is replaced in all other channels by valine, and alanine (eel sequence 1695) is replaced by serine. However, at the core of this peptide the principle of a dipole structure organized as three positively charged amino acids adjacent to two to three negatively charged amino acids is kept, forming the

A C_I^+

Eel	210	Arg⁺-Thr-Phe-Arg⁺-Val-Leu-Arg⁺-Ala-Leu-Lys⁺-Thr-Ile-Thr-Ile
Mus	219	Arg⁺-Thr-Phe-Arg⁺-Val-Leu-Arg⁺-Ala-Leu-Lys⁺-Thr-Ile-Thr-Val
Rat_I	216	Arg⁺-Thr-Phe-Arg⁺-Val-Leu-Arg⁺-Ala-Leu-Lys⁺-Thr-Ile-Ser-Val
Rat_{II}	217	Arg⁺-Thr-Phe-Arg⁺-Val-Leu-Arg⁺-Ala-Leu-Lys⁺-Thr-Ile-Ser-Val
Rat_{III}	216	Arg⁺-Thr-Phe-Arg⁺-Val-Leu-Arg⁺-Ala-Leu-Lys⁺-Thr-Ile-Ser-Val

B Dipole

Eel	1690	Thr-leu-Arg⁺-Arg⁺-Lys⁺-Glu⁻-Glu⁻-Glu⁻-Trp-Ala
Mus	1712	Thr-leu-Arg⁺-Arg⁺-Lys⁺-Gln -Glu⁻-Glu⁻-Val-Ala
Rat_I	1909	Thr-leu-Lys⁺-Arg⁺-Lys⁺-Gln -Glu⁻-Glu⁻-Val-Ser
Rat_{II}	1899	Thr-leu-Lys⁺-Arg⁺-Lys⁺-Gln -Glu⁻-Glu⁻-Val-Ser
Rat_{III}	1845	Thr-leu-Lys⁺-Arg⁺-Lys⁺-Gln -Glu⁻-Glu⁻-Val-Ser

C S_4

S_4I	Arg⁺-Thr-Phe-Arg⁺-Val-Leu-Arg⁺-Ala-Leu-Lys⁺-Thr-Ile-Thr-Ile
S_4IV	Arg⁺-Val-Ile-Arg⁺-Leu-Ala-Arg⁺-Ile-Ala-Arg⁺-Val-Leu-Arg⁺-Leu-Ilu Arg⁺-Ala-Ala-Lys⁺-Gly-Ile-Arg⁺

Fig. 1. Peptide sequence and homology. The sequence of C_I^+ (*A*) and dipole (*B*) of eel electroplax Na channel (top line in *A* and *B*) is compared to the homologous regions of three Na channels from rat brain (Rat I-III) and the Na channel from skeletal muscle (Mus). (*C*) C_I^+ of eel is compared to a peptide S_4IV corresponding to the S_4 region of internal repeat 4 (Tosteson et al., 1989). Numbers to the left represent the corresponding position on the primary amino acid sequence. Dashed line in *A* and *B* represents nonhomologous amino acids. The dipole arrangement in the peptide denoted *dipole* is comprised of the three positively charged amino acids in the middle of the peptide adjacent to 2–3 negatively charged ones.

larger dipole moment *on a sequence* per the entire Na channel molecule.

Antibodies Binding to Purified, Solubilized and Membrane-Bound Na Channels

Antibodies against C_I^+ and dipole bind in a concentration-dependent and specific manner to the corresponding synthetic peptide (Fig. 2*A*). Anti-C_I^+ and anti-dipole did not cross-react with each other (Fig. 2*A* and *B*), indicating their epitope specificity. The specificity of anti-C_I^+ was further evident using the S_4IV peptide (Tosteson, Auld & Tosteson, 1989). Anti-C_I was unreactive with this peptide (Fig. 2*A*) even at dilution as low as 1 : 10 (*not shown*).

The antibodies were found to bind specifically (5–10 times over normal rabbit IgG) to partially purified eel electroplax Na channel and to crude and solubilized eel electroplax membranes.

The antibodies also bind specifically to membrane fraction of excitable tissues prepared from eel electroplax, rat brain and calf heart. In all of these preparations, the binding at 1 : 20 dilution was higher than the binding to the inexcitable tissue of rat liver. The antibodies did not interfere with saxitoxin binding to eel or rat brain membranes.

A mild denaturation of the channel by 0.1% SDS was followed by a significant decrease in binding. This was probably the main reason that the resolution of a 260–270 kD band in immunoblot was very poor (*not shown*). In order to further establish

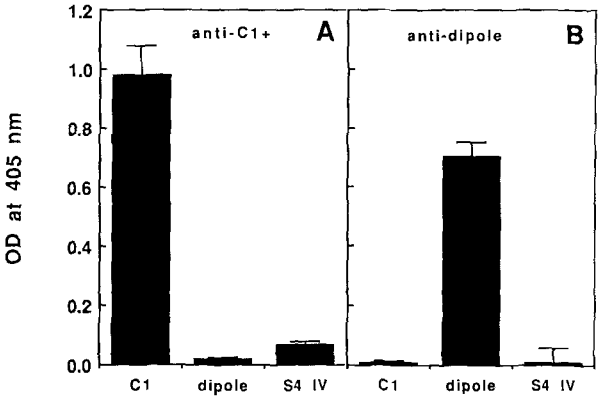

Fig. 2. Antibodies binding to the homologous and heterologous peptides. (*A*) The binding of anti-C_I to C_I, dipole, and S_4IV. (*B*) The binding of anti-dipole to these three peptides. IgG concentrations are 100–200 μg/ml (i.e., the concentration required to obtain 75% of maximal binding to homologous peptides). C_I^+, dipole and S_4IV are the peptides described in Fig. 1. Background binding of normal rabbit IgG was subtracted from each.

the specificity of the antibodies to the Na channel, an immunoprecipitation was performed. Na channels from both eel electroplax (Fig. 3*A* and *C*) and rat brain (Fig. 3*D*), but not from rat liver (Fig. 3*B*), were precipitated by anti-C_I and anti-dipole. Channel precipitation could be prevented by blocking each antibody with the homologous peptide (Fig. 3*C*) or with partially purified channel (*not shown*). Following the immunoprecipitation, the channel

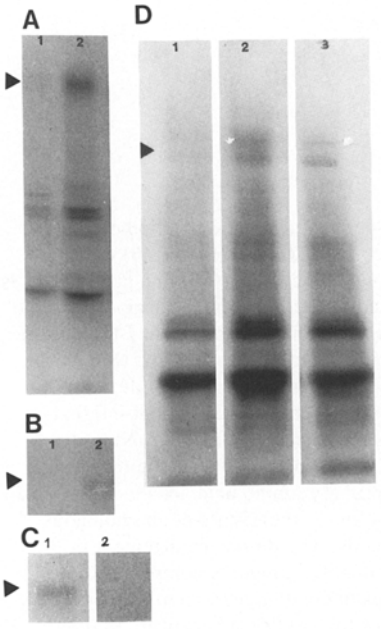

Fig. 3. Immunoprecipitation of Na channels with antibodies. The precipitates were loaded on SDS-PAGE following in-vitro phosphorylation, and the labeled bands were resolved by autoradiography. (*A*) Immunoprecipitation from eel electroplax (lane *1*: normal rabbit IgG; lane *2:* anti-C_I^+). (*B*) Immunoprecipitation from eel electroplax after preadsorption of the antibodies on rat liver membrane (lane *1*: normal rabbit IgG; lane *2*: anti-dipole). (*C*) Immunoprecipitation of eel channel with anti-dipole in the presence (lane *1*) or absence (lane *2*) of the peptide dipole. (*D*) Immunoprecipitation from rat brain (lane *1*: normal rabbit IgG; lane *2*: anti-C_I^+; lane *3*: anti-dipole). Arrowhead is placed at 270 kD in *A–C* and at 260 kD in *D*.

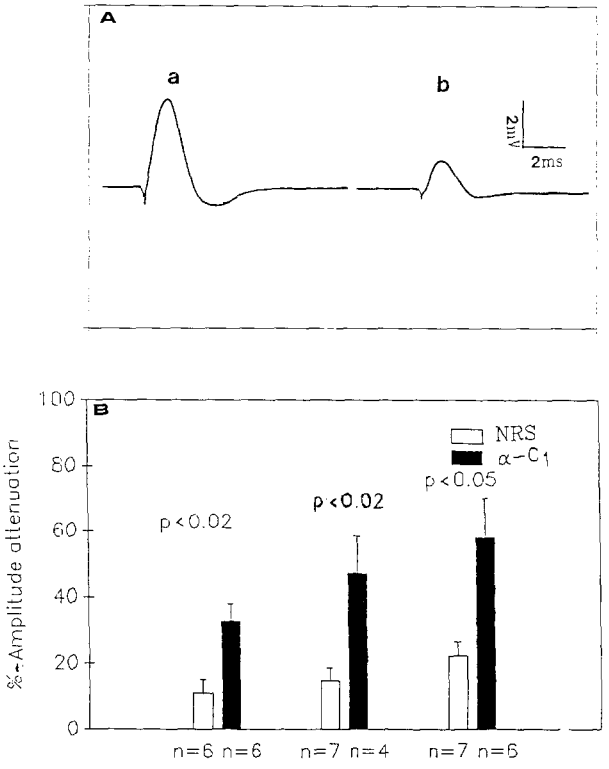

Fig. 4. Electrophysiological modification of the compound action potential in rat sciatic nerve. (*A a*) Control action potential. (*A b*) Twenty min after exposure to 125 μg/ml anti-C_I^+. (*B*) Concentration-dependent attenuation of the action potential amplitude by 50 (left), 100 (middle) and 200 μg/ml (right) of anti-C_I^+ (filled bars) or normal rabbit IgG (open bars). Each point represents the mean of 5–7 nerves.

was detected by in-vitro phosphorylation with cAMP-dependent protein kinase. Phosphorylation of the sodium channel is highly preferential under the employed experimental conditions (Rossie et al., 1987), which results in the presence of a phosphorylated 270-kD band (eel, Fig. 3*A–C*) or 260-kD band (rat brain, Fig. 3*D*). The results shown in Fig. 3 confirm the presence of specific anti-sodium channel antibodies in the antiserum to C_I^+ and dipole. Note that both dipole and C_I^+ domains are far from the phosphorylation sites of cAMP-kinase on the Na channel (Rossie et al., 1987).

The Effects of the Antibodies on the Action Potential

The ability of anti-C_I^+ to specifically increase Na-channel inactivation was previously demonstrated (Meiri et al., 1987, 1989; Schwartz et al., 1990). Na, K or Ca channels were not affected although they were present in the tested preparation (rat DRG cells) (Meiri et al., 1987, 1989). Here we tested the effects of anti-C_I^+ on the action potential of rat sciatic nerve. Anti-C_I^+, but not anti-dipole or normal rabbit IgG, attenuated the action potential amplitude in a concentration-dependent manner (Fig. 4*A* and *B*). Other action potential parameters were not modified (*not shown*). The effect was irreversible when the nerve was subsequently washed for 30–90 min. These results indicate that the C_I^+ domain is accessible to antibodies from the external surface of the membrane and also associated with Na-channel function. The attenuation of action potential amplitude is consistent with the ability of anti-C_I^+ to increase Na-channel inactivation (Meiri et al., 1987, 1989; Schwartz et al., 1990). It is also consistent with the finding of Schwartz et al. (1990) who had demonstrated that anti-C_I^+ works on Na-channel inactivation only when applied externally and not when applied from inside.

Table. Sideness of domain for antibody binding at resting potential

Reagents	Specific binding (cpm/mg protein)		
	Outside	Inside	Perforated
STX	402 ± 11	60 ± 13**	486 ± 13
Anti-C_I^+	4500 ± 545	300 ± 50**	6150 ± 850*
Anti-dipole	800 ± 115	7010 ± 150**	6050 ± 150**

Vesicles of rat brain membranes were loaded with NaPi (for anti-C_I^+) or with KPi (for anti-dipole). The binding of antibodies to the vesicle outside was performed in NaPi buffer. Perforated vesicles were then prepared by 1-hr exposure to 0.05% saponin. Binding to perforated vesicles was performed as described for the binding to the vesicle outside. Binding to the vesicle inside was done by incubating the membranes before vesicle formation with anti-Na channel antibodies followed by vesicle formation and blocking external sites with unlabeled protein A; the vesicles were then washed thoroughly and were exposed to ^{125}I-Protein-A in hypotonic medium. STX binding was performed in parallel on all vesicle preparations to determine the proportion of right-side out vesicles *vs.* inside-out vesicles. At the experiments described in this table, the ratio of outside-out to inside-out was 85 ± 5 : 15 ± 5, and values are given after correction to this ratio. A tight membrane sealing was measured with ^{22}Na loaded inside (for anti-dipole binding) and with ^{86}Rb (for anti-C_I^+ binding). Results are means ± SEM of 3–8 experiments. Values are presented after subtraction of background obtained with normal rabbit IgG in each condition. The background was not affected by saponin and remained 10–15% of the total binding.
* $P < 0.02$; ** $P < 0.002$ for two-tailed unpaired t test (comparison made to the data of each antibody binding to the vesicle outside).

Sideness of the Corresponding Domain and Voltage Dependency of Antibody Binding

Binding at Resting Potential (−70 mV)

First, we measured the antibodies binding to the outside of right-side out vesicles prepared from the membranes of rat brain synaptosomes and kept at −70 mV (Fig. 5*A*, the Table). Antibody binding to the internal side of the vesicles was performed after blocking the external sites on the vesicles with unlabeled protein-A and by lysing of the vesicles with hypotonic solution to expose internal sites (Fig. 5*B*, the Table). Finally, the total binding was determined using perforated vesicles (the Table) obtained by treatment with saponin (Gordon et al., 1987) and by combining the binding to the outside and to the inside of the vesicles. Binding to the external side was corrected for vesicle sideness using STX binding (the Table). At −70 mV (Fig. 5*C*) there was no leakage from the vesicles during 1 hr

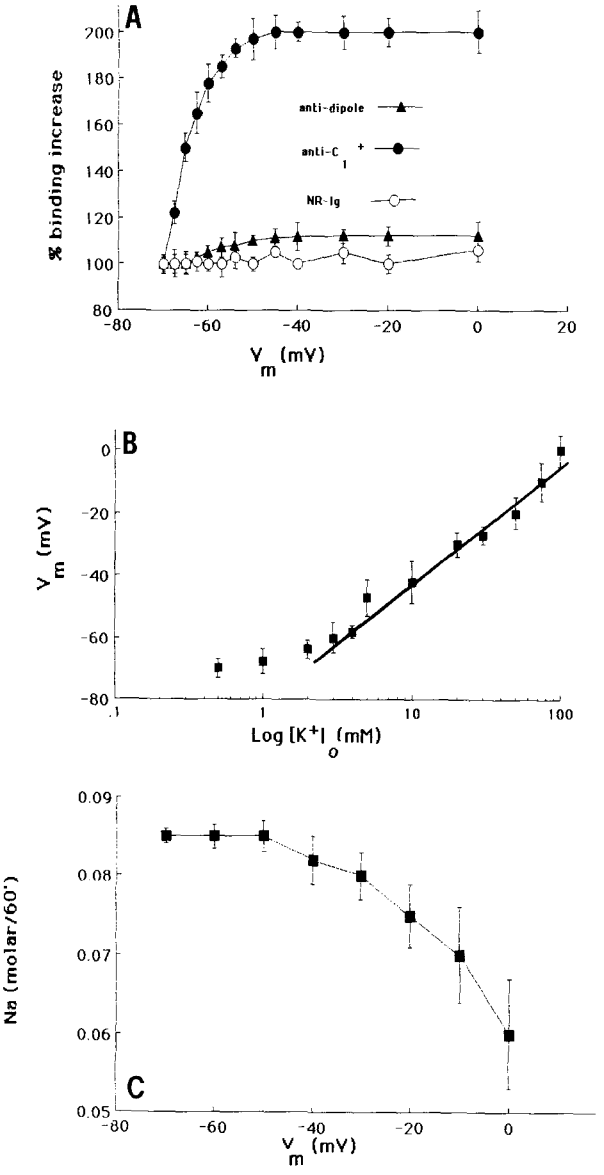

Fig. 5. Voltage-dependent binding of anti-C_I^+ to the outside of the vesicles. (*A*) The binding of antibodies (80–100 μg/ml) to the outside of RBM vesicles. Vesicles are loaded with KPi medium, and binding is performed for 1 hr with NaPi as the test medium containing 5–85 mM NaCl replaced by a balancing concentration of KCl. Sideness is determined by the ^{3}H-STX binding, and values ($\bar{x}$ ± SEM) are shown after correction for this parameter (open circles: normal rabbit IgG; filled circles: anti-C_I^+; open triangles: anti-dipole). (*B*) Membrane potential changes as determined by the [^{3}H]-TPP^+ method is presented as a function of the external potassium concentration with KPi as an internal solution. Values are shown after 1-hr incubation. All values are means of triplicates. Slope: −51, smaller than the anticipated −58 due to nonlinearity at low $[K^+]_o$. (*C*) Measurement of ^{22}Na left in the vesicles as a function of membrane potential. Values are shown after 1-hr incubation. In this figure the test and internal medium contained 1 μM TTX, 10 μM 4AP and 10 mM TEA to avoid radioactive ion transport through sodium and potassium channels opened by depolarization.

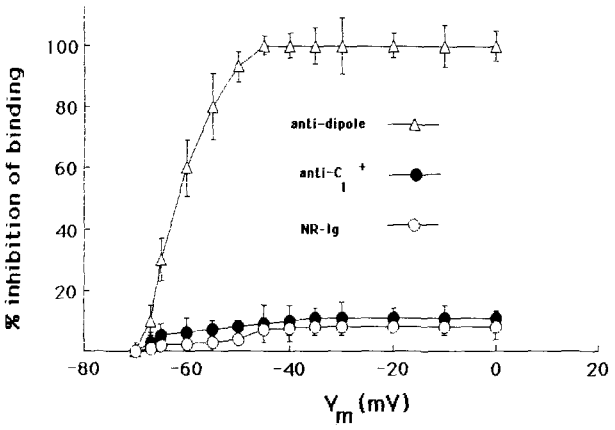

Fig. 6. Voltage-dependent binding to the inside of the vesicles. The binding of antibodies (80–100 μg/ml) to the inside of RBM vesicles was performed. All controls are similar to those described in the Table and Fig. 5. Open circles: normal rabbit IgG; filled circles: anti-C_I^+; open triangles: anti-dipole.

of incubation. The membrane potential (−70 mV), as determined by the TPP^+ method (Fig. 5*B*), was stable during the incubation time.

It was found that at −70 mV anti-C_I^+ binds to the outside of the vesicles (the Table). It has practically no binding (<7%) to the internal side (the Table). Perforating the vesicles by saponin exposes more sites to anti-C_I^+ (50% increase in mean values *vs.* binding to the vesicle outside). Since practically no binding to the vesicles inside was found, the results with anti-C_I indicated that the C_I^+ domain is externally accessible but is at least partially caged inside the membrane bilayer.

The binding of anti-dipole has a different pattern. At −70 mV anti-dipole has eight times more binding sites inside the vesicles than outside (the Table). The binding to the intracellular side is similar to the binding after saponin treatment, indicating that all sites are cytoplasmatic (the Table). The opposite results of the binding of anti-C_I and anti-dipole at resting potential and their comparison to NRS indicate that these values represent differential topography of C_I^+ *vs.* dipole domains in reference to the sideness of the bilayer.

The Effect of Depolarization

The binding of anti-C_I^+ is voltage dependent. Membrane depolarization from −70 to −45 mV increases the binding of anti-C_I^+ to the vesicle outside by a factor of 2 (Fig. 5*A*). This depolarization, however, did not change the very low binding to the vesicle inside (Fig. 6). The controls show that at depolarization from −70 to −40 mV (Fig. 5*B*), the vesicles were tight and no leakage of ^{22}Na was detected at 1-hr incubation (Fig. 5*C*), indicating that the increase in binding is not a result of vesicle breakdown and exposure of internal sites. These results appear to suggest that depolarization increases the accessibility of the C_I^+ domain to the outside.

The voltage dependency of anti-dipole binding is opposite to the voltage dependency of anti-C_I^+ binding. Unlike anti-C_I^+, the binding of anti-dipole to the vesicle outside was neglible at any membrane potential (Fig. 5*A*). However, its binding to the vesicle inside *is* voltage dependent and is completely inhibited by depolarization from −70 to −50 mV (Fig. 6). Vesicle tightness remains unaltered during the experiment (Fig. 5*C*), indicating that depolarization was not causing exposure of internal sites in damaged vesicles.

Discussion

C_I^+ and dipole are two synthetic peptides, 10–13 amino acid long, corresponding to two different domains of the Na channel. These peptides were used to produce site-specific antibodies. The resultant peptide-specific anti-serum recognized Na channels and could immunoprecipitate Na channel from excitable tissue. Specificity was also demonstrated by the lack of interaction between the site-specific antibodies and different domains of the Na channel. Our results demonstrated that the binding of C_I^+ is extracellular and increases by depolarization, whereas the binding of anti-dipole is intracellular and decreases by depolarization. Since these domains are well preserved through evolution, the conclusions related to their voltage-dependent topography have a general importance.

The qualitative differences in the location and recognition of these sodium channel domains as can be summarized from our studies are given in Fig. 7.

Dipole

The accumulated evidence is consistent with a cytoplasmatic location of this domain which becomes less accessible from inside (Fig. 7) upon depolarization. The dipole domain is 60% preserved during evolution (Noda et al., 1984, 1986*a*; Salkoff et al., 1987; Rogart et al., 1989; Kallen et al., 1990). The anti-dipole antibody binds specifically to its corresponding domain. Thus, the effect of depolarization on the accessibility of the dipole domain is both specific and is generally important and relevant to many cloned Na channels.

Dipole domain was localized here to the cytoplasm. This is consistent with the results of Gordon

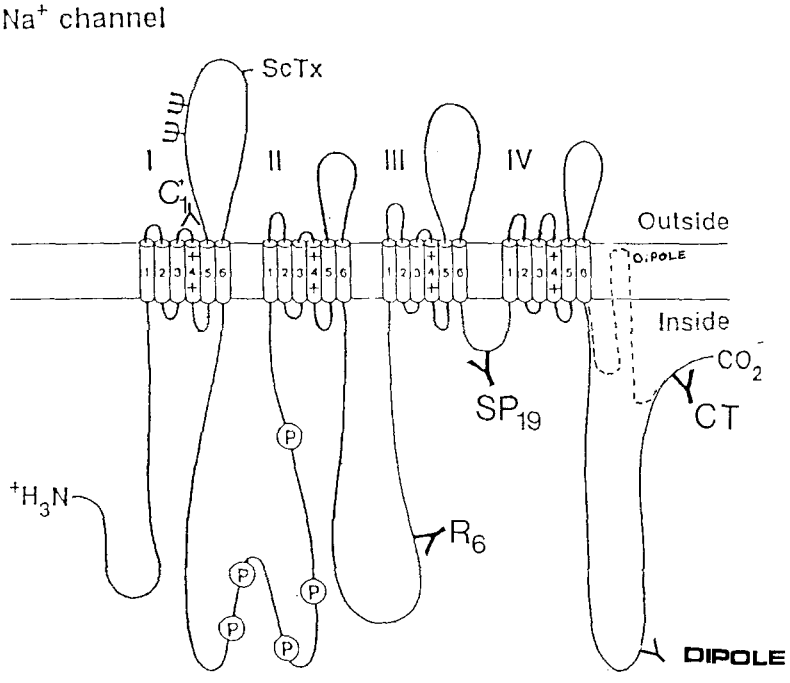

Fig. 7. Schematic sodium channel orientation in the membrane. *I*, *II*, *III*, and *IV* represent the four internal repeats. C_I^+ and *dipole* represent the regions corresponding to our peptides. Note the two putative orientations of dipole. SP_{19} represents the intracellular domain recognized by an antibody which modifies Na-channel inactivation kinetics (Vassilev et al., 1988). R_6 and *CT* represent regions mapped in immunocytochemistry to the cytoplasmatic side (Gordon et al., 1987, 1988). *P* represents potential phosphorylation sites in rat brain Na channels (Rossie et al., 1987). *ScTx* represents the localized site for scorpion toxin (Catterall, 1988; Trimmer et al., 1989) and TTX (Catterall, 1990; Stuhmer, 1990). Segment *4* of *I*—the region recognized as the voltage sensor (Stuhmer et al., 1989). The scheme was modified from Catterall (1988).

et al. (1987) who showed the cytoplasmatic location of the C-terminus of the Na channel. Yet, at depolarization the accessibility of dipole domain from inside diminished, and no changes upon depolarization are found at the membrane outside. One potential assumption is that upon depolarization the dipole domain becomes "superpacked" at the cytoplasm. Such superpacking is not very likely. The electric field is significantly diminished in solution, and a voltage difference of −70 mV across the membrane is decreased to a fraction of a millivolt over a distance less than a nanometer in a solution of 100–150 mM (Miller, 1986). This makes the superpacking assumption not very appealing.

Is it possible that the cytoplasmatic dipole domain becomes inserted in the plasma membrane upon depolarization? Dipole is constructed as three positively charged amino acids continued on a sequence with three negatively charged amino acids, thus building the larger dipole moment on a sequence for the entire Na channel molecule. If dipole is positioned underneath to the plasma membrane, depolarization may "sink" the negative charges inside the bilayer and make the region less accessible for antibodies. However, dipole is highly hydrophilic, and it seems improbable that such a domain will enter the transmembrane region.

A third assumption is therefore suggested. This assumption attributes the inhibited binding of anti-dipole by depolarization to an allosteric effect. The intracellular region between repeats 3 and 4 is involved in inactivation (Vassilev et al., 1988; Stuhmer et al., 1989). Several groups suggested that the segment following internal repeat 4 (to which the dipole domain belongs) is also associated with inactivation (Noda et al., 1984; Guy, 1987; Salkoff et al., 1987). Guy has postulated that when the channel is inactivated, the segment between repeats 3 and 4 binds to the internal segment following repeat 4 (to which dipole belongs). If his hypothesis is correct, it is anticipated that when the channel is inactivated by prolonged depolarization, the intracellular segment between repeats 3 and 4 bind to the dipole intracellular segment and make it unavailable to antibodies. This may explain the voltage-dependent decrease of the binding of anti-dipole. This intriguing assumption could now be tested in several ways: (i) There are drugs and toxins that prevent inactivation which can be used to study if they can eliminate the voltage-dependent binding of anti-dipole. (ii) Application of anti-dipole from inside in patch-clamp studies may modify Na-channel inactivation. (iii) In channel mutants that lack the segment between repeat 3 and 4, the voltage-dependent binding of anti-dipole is expected to be missing. All of these are currently being tested in our lab.

C_I^+

The accessibility of the C_I^+ domain to antibodies applied to the external membrane surface was demonstrated for at least three different excitable tissues—rat peripheral nerve (this work), cultured DRG cells (Schwartz et al., 1990) and vesicles of rat

brain synaptosomes (this work). Considering the conservation of the C_I^+ domain among various excitable tissues (Fig. 1*A*), the implication of external accessibility of the C_I^+ domain in mature excitable cells is rather general. Yet C_I^+ is a part of the S_4 region of internal repeat 1 identified as the voltage sensor of the Na channel (Stuhmer et al., 1989) which is expected to be in the membrane bilayer (Armstrong, 1981; Kosower, 1985, 1991; Catterall, 1988; Guy & Conti, 1990). It is interesting that in this study we found that upon depolarization the C_I^+ region becomes more accessible to antibodies. The results are consistent with the conclusion that a part of the conformational changes associated with membrane depolarization involves the exposure of the voltage sensor to the extracellular solution. The results are consistent with the finding of Schwartz et al. (1990) which have shown that antibodies to C_I^+ specifically modulate Na current only from outside and not from inside. Further support to the accessibility of the S_4 domain of internal repeat 1 (designated here as the C_I^+ domain) to the extracellular solution upon depolarization was shown by Pusch (1990). A mutation of the S_4 lysine to glutamine in the fourth positively charged position altered blockade of the sodium channel by extracellular calcium, but did not affect channel blockade by intracellular magnesium (Pusch, 1990). These results indicate that this region becomes accessible to the extracellular solution upon depolarization (Pusch, 1990). Our results also provide experimental support to the propagating helix model suggested by Guy and Conti (1990). According to their model, the first four positive charges of the S_4 regions become exposed at membrane depolarization. Based on all studies, the C_I^+ domain, which includes all four positive charges of the S_4 region of internal repeat 1, is postulated to move outside at depolarization and, thereby, becomes more accessible to antibodies. These findings might also be relevant to other voltage-gated cation channels since the S_4 segment appears in all of them. Yet, anti-C_I^+ work specifically on the S_4 segment of internal repeat 1 and does not recognize other S_4 segments of the Na channels. Thus, to study voltage-dependent conformational changes at S_4 segments of Na and other cation channels, more antibodies should be generated.

The employment of immunological markers has been very helpful in providing information regarding the three-dimensional configuration of the sodium channel in the membrane (Barchi, 1988; Catterall, 1990). Combinations of immunological techniques, site-directed mutagenesis coupled to functional expression systems and x-ray diffraction of the channel may make it possible to identify all these sites in the nearby future.

We are most grateful to Dr. M.T. Tosteson (Harvard Medical School) for providing us with samples of the S_4IV peptides. We wish to express our gratitude to Drs. D. Gordon (Hebrew University) and A. Safran (The Weizmann Institute) for helping in the immunoprecipitation procedure, to Drs. H. Rahamimoff (Hebrew University) and A. Barzilai (Columbia University) for advising us with the vesicle experiments, to Drs. D. Kassel and M. Gavish (Technion) for many fruitful discussions, and to Dr. Y. Palti (Technion) for discussions of electric field and suggesting the dipole peptide. This work was supported by a basic research fund (BRF) of The Israel Academy of Sciences #430.87 (H.M. and G.S.), a BSF Grant #84-00367 (H.M.) and The Henry Gutwirt Fund for the Promotion of Research-Technion VPR Fund #184-0093 (H.M.).

References

Agnew, W.S., Rosenberg, R.L., Tomiko, S.A. 1986. Reconstitution of the sodium channels from *Electrophorus electricus*. *In*: Ion Channel Reconstitution. C. Miller, editor. pp. 307–336. Plenum, New York

Aldrich, R.W., Stevens, C.F. 1987. Voltage dependent gating of sodium channels from mammalian neuroblastoma cells. *J. Neurosci.* **7**:418–431

Armstrong, C.M. 1981. Sodium currents and gating currents. *Physiol. Rev.* **61**:644–683

Barchi, R.L. 1988. Probing the molecular structure of the voltage dependent sodium channel. *Annu. Rev. Neurosci.* **11**:455–495

Barzilai, A., Rahamimoff, H. 1987. Stoichiometry of sodium-calcium exchanges in nerve terminals. *Biochemistry* **26**:6113–6118

Bezanilla, F. 1985. Gating of sodium and potassium channels. *J. Membrane Biol.* **88**:97–111

Bruns, R.F., Lawson-Wendling, K., Pugsley, T.A. 1983. A rapid filtration assay for soluble receptors using polyethylen amine-treated filters. *Anal. Biochem.* **132**:74–81

Caldwell, J.H., Schaller, K.L. 1989. Isolation of novel Na channel genes by PCR gene amplification. *Soc. Neurosci.* **15**:197*a*

Catterall, W.A. 1988. Structure and function of voltage sensitive ion channels. *Science* **242**:50–61

Catterall, W.A. 1990. Molecular properties of voltage sensitive Na^+ and Ca^{++} channels. *Biophys. J.* **57**:195*a*

Costa, M.R., Catterall, W.A. 1984. Cyclic AMP-dependent phosphorylation of the alpha subunit of the sodium channel in synaptic nerve ending particles. *J. Biol. Chem.* **259**:8210–8218

Duch, D.S., Levinson, S.R. 1987. Neurotoxin modulated uptake of sodium by highly purified preparation of the electroplax tetrodotoxin binding glycoprotein reconstituted into lipid vesicles. *J. Membrane Biol.* **98**:43–55

Ganetzki, B., Loughney, K. 1989. Alternative splicing generates distinct sodium channel subtypes in *Drosophila*. *Soc. Neurosci.* **15**:196*a*

Gasko, D.D., Knowles, A.F., Shertzer, H.C., Suolinna, E.H., Racker, E. 1976. The use of ion exchange resins for studying ion channel transport in biological systems. *Anal. Biochem.* **72**:57–65

Gordon, R.D., Fieles, W.E., Schotland, D.L., Hogue-Angeletti, R., Barchi, R.L. 1987. Topographical localization of the C-terminal of the voltage-dependent sodium channel from *Electrophorus electricus* using antibodies raised against a synthetic peptide. *Proc. Natl. Acad. Sci. USA* **84**:308–312

Gordon, R.D., Li, Y., Fieles, W.E., Schotland, D.L., Barchi, R.L. 1988. Topological localization of a segment of the eel voltage dependent sodium channel primary sequence (AA 927-938) that discriminates models of tertiary structure. *J. Neurosci.* **8**:3742–3749

Greenblatt, R.E., Blatt, Y., Montal, M. 1985. The structure of the voltage sensitive sodium channels. Inferences derived from computer-aided analysis of the *Electrophorus electricus* channel primary structure. *FEBS Lett.* **193**:125–134

Guy, H.R. 1987. How sodium channels work—a molecular model. *Curr. Topics Membr. Transp.* **33**:289–308

Guy, H.R., Conti, F. 1990. Pursuing the structure and function of voltage-gated channels. *Trends Neurosci.* **13**:201–206

Guy, H.R., Seetharamulu, P. 1986. Molecular model of the action potential sodium channel. *Proc. Natl. Acad. Sci. USA* **83**:508–512

Hille, B. 1984. Ionic Channels of Excitable Membrane. pp. 426. Sinauer, Sunderland (MA)

Hodgkin, A.L., Huxley, A.F. 1952. A quantitative description of membrane current and its application to conduction and excitation in nerve. *J. Physiol.* **116**:500–544

Kallen, R.G., Sheng, Z., Yank, J., Chen, L.Q., Fishbeck, K., Barchi, R.L. 1990. Primary structure and expression of a sodium channel characteristic of denervated and immature rat skeletal muscle. *Neuron* **4**:233–242

Kanner, B.I. 1980. Modulation of neurotransmitter transport by the activity of the action potential sodium ion in membrane vesicles from rat. *Biochemistry* **19**:692–697

Kayano, T., Noda, M., Flockerzi, V., Takahashi, A., Numa, S. 1988. Primary structure of the rat brain sodium channel III deduced from the cDNA sequence. *FEBS Lett.* **228**:187–194

Kosower, E.M. 1985. A structural and dynamic molecular model for the sodium channel of *Electrophorus electricus*. *FEBS Lett.* **182**:235–242

Kosower, E.M. 1991. Structure and dynamic molecular models for sodium channels. *In*: The Molecular Basis of Learning and Memory. Princeton University Press (*in press*)

Laemmli, U.K. 1970. Cleavage of structural proteins during the assembly of the head of bacteriophage T_4. *Nature* **227**:680–685

Levinson, S.R., Duch, S.D., Urban, B.W., Recio-Pinto, E. 1986. The sodium channels from *Electrophorus electricus*. *Ann. NY Acad. Sci.* **479**:162–178

Lombet, A., Lazdunski, M. 1984. Characterization, solubilization, affinity labeling and purification of the cardiac sodium channel using *Tityus* toxin gamma. *Eur. J. Biochem.* **141**:651–660

Lowry, O.H., Rosenbrough, N.J., Farr, R.J., Randall, J. 1951. Protein measurement with the folin-phenol reagent. *J. Biol. Chem.* **193**:265–275

Meiri, H., Sammar, M., Schwartz, A. 1989. Production and use of synthetic peptide antibodies to map a region associated with sodium channel inactivation. Immunological techniques: Anti-idiotype antibodies and molecular mimicry. *Methods Enzymol.* **178**:714–739

Meiri, H., Spira, G., Sammar, M., Namir, M., Schwartz, A., Komoriya, A., Kosower, E.M., Palti, Y. 1987. Mapping a region associated with Na channel inactivation using antibodies to a synthetic peptide corresponding to a part of the channel. *Proc. Natl. Acad. Sci. USA* **84**:5058–5062

Merrifield, R.B. 1985. Solid phase synthesis. *Angew. Chem. Int. Ed. Engl.* **24**:799–810

Miller, C.M. 1986. How ion channel proteins work. *In*: Neuromodulation: The Biochemical Control of Neuronal Excitability. L.K. Kaczmarek and I.B. Levitan, editor. Chap. 3, pp. 39–55. Oxford University Press, New York

Noda, M., Idada, T., Suzuki, H., Takeshima, H., Takahashi, T., Kuno, M., Numa, S. 1986*a*. Expression of functional sodium channels from cloned cDNA. *Nature* **322**:826–828

Noda, M., Ikeda, T., Kayano, T., Suzuki, H., Takeshima, H., Kurasaki, M., Takahashi, H., Numa, S. 1986*b*. Existence of distinct sodium channel messenger RNA in rat brain. *Nature* **320**:188–192

Noda, M., Shimizu, S., Tanabe, T., Takai, T., Kayano, T., Ikeda, T., Takahashi, H., Nakayama, H., Kanaoka, Y., Miniamino, N., Kangawa, K., Matsuo, H., Raftery, M.A., Hirose, T., Inayama, S., Hayashida, H., Miyata, T., Numa, S. 1984. Primary structure of *Electrophorus electricus* sodium channel deduced from cDNA sequence. *Nature* **312**:121–127

Pusch, M. 1990. Block of different cloned Na-channels by internal Mg^{++} and external Ca^{++}. *Biophys. J.* **57**:105*a*

Reeves, S., Sutko, J.L. 1979. Na-Ca ion exchange in cardiac membrane vesicles. *Biochemistry* **76**:590–594

Rogart, R.B., Cribbs, L.L., Muglia, L.K., Kephalp, D.D., Kaiser, M.W. 1989. Molecular cloning of a putative TTX-resistant rat heart Na channel isoform. *Proc. Natl. Acad. Sci. USA* **86**:8170–8174

Rossie, S., Gordon, D., Catterall, W.A. 1987. Identification of an intracellular domain of the sodium channel having multiple cAMP-dependent phosphorylation sites. *J. Biol. Chem.* **262**:17530–17539

Salkoff, L., Butler, A., Wei, A., Scavarda, N., Baker, K., Pauron, D., Smith, C. 1987. *Trends Neurosci.* **10**:522–527

Salkoff, L., Butler, A., Wei, A., Scavarda, N., Giffen, K., Ilfune, C., Goodman, R., Mandel, G. 1987. Genomic organization and deduced amino acids sequence of a putative sodium channel gene in *Drosophila*. *Science* **237**:744–748

Schwartz, A., Palti, Y., Meiri, H. 1990. Structural and developmental differences between 3 types of Na channels in dorsal root ganglion of newborn rats. *J. Membrane Biol.* **116**:117–128

Stuhmer, W. 1990. Site directed mutagenesis on voltage gated channels. *Biophys. J.* **57**:386*a*

Stuhmer, W., Conti, F., Suzuki, H., Wang, X., Noda, M., Yahagi, N., Kubo, H., Numa, S. 1989. Structural parts involved in activation and inactivation of the sodium channel. *Nature* **339**:597–603

Suzuki, H., Beckh, S., Kubo, H., Yahagi, N., Ishida, H., Kayano, T., Noda, M., Numa, S. 1988. Functional expression of cloned cDNA encoding sodium channel III. *FEBS Lett.* **228**:195–200

Tosteson, M.T., Auld, D.S., Tosteson, D.C. 1989. Voltage gated channels formed in lipid bilayers by a positively charged segment of the Na-channel polypeptide. *Proc. Natl. Acad. Sci. USA* **86**:707–710

Trimmer, S., Jr., Cooperman, S.S., Tomiko, S.A., Zhou, J., Crean, S.M., Boyk, M.B., Galle, R.G., Sheng, Z., Barchi, R.L., Sigworth, F.J., Goodman, R.H., Agnew, W.S., Mandel, G. 1989. Primary structure and functional expression of a mammalian skeletal muscle sodium channel. *Neuron* **3**:33–49

Vassilev, P.M., Scheur, T., Catterall, W.A. 1988. Identification of an intracellular peptide segment involved in sodium channel inactivation. *Science* **241**:1658–1660

Wray, W., Boulikas, T., Wray, V.P., Hancock, R. 1981. Silver staining of proteins in polyacrylamid gels. *Anal. Biochem.* **118**:197–203

Received 24 May 1990; revised 2 April 1991